

Bottom photoproduction measured using decays into muons in dijet events in ep collisions at $\sqrt{s}=318$ GeV

S. Chekanov, M. Derrick, D. Krakauer, J. H. Loizides,^a S. Magill, S. Miglioranza,^a B. Musgrave, J. Repond, and R. Yoshida
Argonne National Laboratory, Argonne, Illinois 60439-4815, USA

M. C. K. Mattingly
Andrews University, Berrien Springs, Michigan 49104-0380, USA

P. Antonioli, G. Bari, M. Basile, L. Bellagamba, D. Boscherini, A. Bruni, G. Bruni, G. Cara Romeo, L. Cifarelli,
F. Cindolo, A. Contin, M. Corradi, S. De Pasquale, P. Giusti, G. Iacobucci, A. Margotti, A. Montanari, R. Nania, F. Palmonari,
A. Pesci, G. Sartorelli, and A. Zichichi
University of Bologna and INFN Bologna, Bologna, Italy

G. Aghuzumtsyan, D. Bartsch, I. Brock, S. Goers, H. Hartmann, E. Hilger, P. Irrgang, H.-P. Jakob, O. Kind, U. Meyer,
E. Paul, J. Rautenberg, R. Renner, A. Stifutkin, J. Tandler, K. C. Voss, M. Wang, and A. Weber
Physikalisches Institut der Universität Bonn, Bonn, Germany

D. S. Bailey, N. H. Brook, J. E. Cole, G. P. Heath, T. Namssoo, S. Robins, and M. Wing
H.H. Wills Physics Laboratory, University of Bristol, Bristol, United Kingdom

M. Capua, A. Mastroberardino, M. Schioppa, and G. Susinno
Calabria University, Physics Department and INFN, Cosenza, Italy

J. Y. Kim, Y. K. Kim, J. H. Lee, I. T. Lim, and M. Y. Pac^b
Chonnam National University, Kwangju, Korea

A. Caldwell,^c M. Helbich, X. Liu, B. Mellado, Y. Ning, S. Paganis, Z. Ren, W. B. Schmidke, and F. Sciulli
Nevis Laboratories, Columbia University, Irvington on Hudson, New York 10027

J. Chwastowski, A. Eskreys, J. Figiel, A. Galas, K. Olkiewicz, P. Stopa, and L. Zawiejski
Institute of Nuclear Physics, Cracow, Poland

L. Adamczyk, T. Bołd, I. Grabowska-Bołd, D. Kisiełowska, A. M. Kowal, M. Kowal, T. Kowalski, M. Przybycień,
L. Suszycki, D. Szuba, and J. Szuba
Faculty of Physics and Nuclear Techniques, AGH–University of Science and Technology, Cracow, Poland

A. Kotański and W. Słomiński
Department of Physics, Jagellonian University, Cracow, Poland

V. Adler, U. Behrens, I. Bloch, K. Borras, V. Chiochia, D. Dannheim, G. Drews, J. Fourletova, U. Fricke, A. Geiser,
P. Göttlicher,^d O. Gutsche, T. Haas, W. Hain, S. Hillert,^e B. Kahle, U. Kötz, H. Kowalski,^f G. Kramberger, H. Labes, D. Lelas,
H. Lim, B. Lühr, R. Mankel, I.-A. Melzer-Pellmann, C. N. Nguyen, D. Notz, A. E. Nuncio-Quiroz, A. Polini,
A. Raval, L. Rurua, U. Schneekloth, U. Stösslein, G. Wolf, C. Youngman, and W. Zeuner
Deutsches Elektronen-Synchrotron DESY, Hamburg, Germany

S. Schlenstedt
DESY Zeuthen, Zeuthen, Germany

G. Barbagli, E. Gallo, C. Genta, and P. G. Pelfer
University of Florence and INFN, Florence, Italy

A. Bamberger, A. Benen, F. Karstens, D. Dobur, and N. N. Vlasov
Fakultät für Physik der Universität Freiburg i.Br., Freiburg i.Br., Germany

M. Bell, P. J. Bussey, A. T. Doyle, J. Ferrando, J. Hamilton, S. Hanlon, D. H. Saxon, and I. O. Skillicorn
Department of Physics and Astronomy, University of Glasgow, Glasgow, United Kingdom

I. Gialas

Department of Engineering in Management and Finance, University of Aegean, Greece

T. Carli, T. Gosau, U. Holm, N. Krumnack, E. Lohrmann, M. Milite, H. Salehi, P. Schleper, S. Stonjek,^c K. Wichmann,
K. Wick, A. Ziegler, and Ar. Ziegler
Hamburg University, Institute of Exp. Physics, Hamburg, Germany

C. Collins-Tooth, C. Foudas, R. Gonçalo,^g K. R. Long, and A. D. Tapper
Imperial College London, High Energy Nuclear Physics Group, London, United Kingdom

P. Cloth and D. Filges

Forschungszentrum Jülich, Institut für Kernphysik, Jülich, Germany

M. Kataoka,^h K. Nagano, K. Tokushuku,ⁱ S. Yamada, and Y. Yamazaki
Institute of Particle and Nuclear Studies, KEK, Tsukuba, Japan

A. N. Barakbaev, E. G. Boos, N. S. Pokrovskiy, and B. O. Zhautykov
Institute of Physics and Technology of Ministry of Education and Science of Kazakhstan, Almaty, Kazakhstan

D. Son

Kyungpook National University, Center for High Energy Physics, Daegu, South Korea

K. Piotrkowski

Institut de Physique Nucléaire, Université Catholique de Louvain, Louvain-la-Neuve, Belgium

F. Barreiro, C. Glasman, O. González, L. Labarga, J. del Peso, E. Tassi, J. Terrón, M. Vázquez, and M. Zambrana
Departamento de Física Teórica, Universidad Autónoma de Madrid, Madrid, Spain

M. Barbi, F. Corriveau, S. Gliga, J. Lainesse, S. Padhi, D. G. Stairs, and R. Walsh
Department of Physics, McGill University, Montréal, Québec H3A 2T8, Canada

T. Tsurugai

Meiji Gakuin University, Faculty of General Education, Yokohama, Japan

A. Antonov, P. Danilov, B. A. Dolgoshein, D. Gladkov, V. Sosnovtsev, and S. Suchkov
Moscow Engineering Physics Institute, Moscow, Russia

R. K. Dementiev, P. F. Ermolov, Yu. A. Golubkov,^j I. I. Katkov, L. A. Khein, I. A. Korzhavina, V. A. Kuzmin,
B. B. Levchenko, O. Yu. Lukina, A. S. Proskuryakov, L. M. Shcheglova, and S. A. Zotkin
Moscow State University, Institute of Nuclear Physics, Moscow, Russia

N. Coppola, S. Grippink, E. Koffeman, P. Kooijman, E. Maddox, A. Pellegrino, S. Schagen, H. Tiecke, J. J. Velthuis,
L. Wiggers, and E. de Wolf
NIKHEF and University of Amsterdam, Amsterdam, Netherlands

N. Brümmer, B. Bylsma, L. S. Durkin, and T. Y. Ling
Physics Department, Ohio State University, Columbus, Ohio 43210

A. M. Cooper-Sarkar, A. Cottrell, R. C. E. Devenish, B. Foster, G. Grzelak, C. Gwenlan, S. Patel, P. B. Straub,
and R. Walczak
Department of Physics, University of Oxford, Oxford, United Kingdom

A. Bertolin, R. Brugnera, R. Carlin, F. Dal Corso, S. Dusini, A. Garfagnini, S. Limentani, A. Longhin, A. Parenti,
M. Posocco, L. Stanco, and M. Turcato
Dipartimento di Fisica dell'Università and INFN, Padova, Italy

E. A. Heaphy, F. Metlica, B. Y. Oh, and J. J. Whitmore^k
Department of Physics, Pennsylvania State University, University Park, Pennsylvania 16802

Y. Iga

Polytechnic University, Sagamihara, Japan

G. D'Agostini, G. Marini, and A. Nigro

Dipartimento di Fisica, Università 'La Sapienza' and INFN, Rome, Italy

C. Cormack,¹ J. C. Hart, and N. A. McCubbin

Rutherford Appleton Laboratory, Chilton, Didcot, Oxon, United Kingdom

C. Heusch

University of California, Santa Cruz, California 95064, USA

I. H. Park

Department of Physics, Ewha Womans University, Seoul, Korea

N. Pavel

Fachbereich Physik der Universität-Gesamthochschule Siegen, Germany

H. Abramowicz, A. Gabareen, S. Kananov, A. Kreisel, and A. Levy

Raymond and Beverly Sackler Faculty of Exact Sciences, School of Physics, Tel-Aviv University, Tel-Aviv, Israel

M. Kuze

Department of Physics, Tokyo Institute of Technology, Tokyo, Japan

T. Fusayasu, S. Kagawa, T. Kohno, T. Tawara, and T. Yamashita

Department of Physics, University of Tokyo, Tokyo, Japan

R. Hamatsu, T. Hirose, M. Inuzuka, H. Kaji, S. Kitamura,^m and K. Matsuzawa

Tokyo Metropolitan University, Department of Physics, Tokyo, Japan

M. I. Ferrero, V. Monaco, R. Sacchi, and A. Solano

Università di Torino and INFN, Torino, Italy

M. Arneodo and M. Ruspa

Università del Piemonte Orientale, Novara, and INFN, Torino, Italy

T. Koop, J. F. Martin, and A. Mirea

Department of Physics, University of Toronto, Toronto, Ontario M5S 1A7, Canada

J. M. Butterworth,ⁿ R. Hall-Wilton, T. W. Jones, M. S. Lightwood, M. R. Sutton, and C. Targett-Adams

Physics and Astronomy Department, University College London, London, United Kingdom

J. Ciborowski,^o R. Ciesielski, P. Łuźniak,^p R. J. Nowak, J. M. Pawlak, J. Sztuk,^q T. Tymieniecka, A. Ukleja, J. Ukleja,
and A. F. Zarnecki

Warsaw University, Institute of Experimental Physics, Warsaw, Poland

M. Adamus and P. Plucinski

Institute for Nuclear Studies, Warsaw, Poland

Y. Eisenberg, L. K. Gladilin,^r D. Hochman, U. Karshon, and M. Riveline

Department of Particle Physics, Weizmann Institute, Rehovot, Israel

D. Kçira, S. Lammers, L. Li, D. D. Reeder, M. Rosin, A. A. Savin, and W. H. Smith

Department of Physics, University of Wisconsin, Madison, Wisconsin 53706, USA

A. Deshpande and S. Dhawan

Department of Physics, Yale University, New Haven, Connecticut 06520-8121, USA

S. Bhadra, C. D. Catterall, S. Fourletov, G. Hartner, S. Menary, M. Soares, and J. Standage
Department of Physics, York University, Ontario M3J 1P3, Canada

(ZEUS Collaboration)

(Received 23 December 2003; published 30 July 2004)

The photoproduction of bottom quarks in events with two jets and a muon has been measured with the ZEUS detector at HERA using an integrated luminosity of 110 pb^{-1} . The fraction of jets containing b quarks was extracted from the transverse momentum distribution of the muon relative to the closest jet. Differential cross sections for bottom production as a function of the transverse momentum and pseudorapidity of the muon, of the associated jet and of x_{γ}^{jets} , the fraction of the photon's momentum participating in the hard process, are compared with MC models and QCD predictions made at next-to-leading order. The latter give a good description of the data.

DOI: 10.1103/PhysRevD.70.012008

PACS number(s): 13.60.-r, 14.40.Lb, 12.38.Qk

I. INTRODUCTION

The production of bottom quarks in ep collisions at HERA is a stringent test for perturbative quantum chromodynamics (QCD) since the large b -quark mass ($m_b \sim 5 \text{ GeV}$) provides a hard scale that should ensure reliable predictions. When Q^2 , the negative squared four-momentum exchanged at the electron vertex, is small the reaction $ep \rightarrow e' b \bar{b} X$ can be considered as a photoproduction process in which a quasi-real photon, emitted by the incoming electron, interacts with the proton.

For b -quark transverse momenta comparable to the b -quark mass, next-to-leading-order (NLO) QCD calculations in which the b quark is generated dynamically are expected to provide accurate predictions for b photoproduction [1]. The corresponding leading-order (LO) QCD processes are the direct-photon process, in which the quasi-real photon enters directly in the hard interaction, $\gamma g \rightarrow b \bar{b}$, and the

resolved-photon process, in which the photon acts as a source of partons that take part in the hard interaction ($gg \rightarrow b \bar{b}$ or $q \bar{q} \rightarrow b \bar{b}$).

The bottom-production cross section has been measured in $p\bar{p}$ collisions at the ISR [2], $Sp\bar{p}S$ [3] and Tevatron colliders [4], in $\gamma\gamma$ interactions at LEP [5] and in fixed-target πN [6] and pN [7] experiments. Apart from the $Sp\bar{p}S$ data and the fixed-target experiments, the results were significantly above the NLO QCD prediction. The H1 measurement in ep interactions at HERA [8] found a cross section significantly larger than the prediction. The previous ZEUS measurement [9] was above, but consistent with, the prediction.

This paper reports a measurement of bottom photoproduction in events with two jets and a muon, $ep \rightarrow e' b \bar{b} X \rightarrow e' jj\mu X'$, for $Q^2 < 1 \text{ GeV}^2$.

II. EXPERIMENTAL SETUP

The data sample used in this analysis corresponds to an integrated luminosity $\mathcal{L} = 110.4 \pm 2.2 \text{ pb}^{-1}$, collected by the ZEUS detector in the years 1996–1997 and 1999–2000. During the 1996–1997 data taking, HERA provided collisions between an electron¹ beam of $E_e = 27.5 \text{ GeV}$ and a proton beam of $E_p = 820 \text{ GeV}$, corresponding to a center-of-mass energy $\sqrt{s} = 300 \text{ GeV}$ ($\mathcal{L}_{300} = 38.0 \pm 0.6 \text{ pb}^{-1}$). In the years 1999–2000, the proton-beam energy was $E_p = 920 \text{ GeV}$, corresponding to $\sqrt{s} = 318 \text{ GeV}$ ($\mathcal{L}_{318} = 72.4 \pm 1.6 \text{ pb}^{-1}$).

A detailed description of the ZEUS detector can be found elsewhere [10]. A brief outline of the components that are most relevant for this analysis is given below.

Charged particles are tracked in the central tracking detector (CTD) [11], which operates in a magnetic field of 1.43 T provided by a thin superconducting solenoid. The CTD consists of 72 cylindrical drift chamber layers, organized in nine superlayers covering the polar-angle² region $15^\circ < \theta$

^aAlso affiliated with University College London, London, UK.

^bNow at Dongshin University, Naju, Korea.

^cNow at Max-Planck-Institut für Physik, München, Germany.

^dNow at DESY group FEB.

^eNow at University of Oxford, Oxford, UK.

^fOn leave of absence at Columbia University, Nevis Labs., NY, USA.

^gNow at Royal Holloway University of London, London, UK.

^hAlso at Nara Women's University, Nara, Japan.

ⁱAlso at University of Tokyo, Tokyo, Japan.

^jNow at HERA-B.

^kOn leave of absence at The National Science Foundation, Arlington, VA, USA.

^lNow at University of London, Queen Mary College, London, UK.

^mPresent address: Tokyo Metropolitan University of Health Sciences, Tokyo 116-8551, Japan.

ⁿAlso at University of Hamburg, Alexander von Humboldt Fellow.

^oAlso at Łódź University, Poland.

^pŁódź University, Poland.

^qŁódź University, Poland.

^rOn leave from MSU.

¹Electrons and positrons are not distinguished in this paper and are both referred to as electrons.

²The ZEUS coordinate system is a right-handed Cartesian system,

$<164^\circ$. The transverse-momentum resolution for full-length tracks is $\sigma(p_T)/p_T = 0.0058 p_T \oplus 0.0065 \oplus 0.0014/p_T$, with p_T in GeV.

The high-resolution uranium-scintillator calorimeter (CAL) [12] consists of three parts: the forward (FCAL), the barrel (BCAL) and the rear (RCAL) calorimeters. Each part is subdivided transversely into towers and longitudinally into one electromagnetic section (EMC) and either one (in RCAL) or two (in BCAL and FCAL) hadronic sections (HAC). The smallest subdivision of the calorimeter is called a cell. The CAL energy resolutions, as measured under test-beam conditions, are $\sigma(E)/E = 0.18/\sqrt{E}$ for electrons and $\sigma(E)/E = 0.35/\sqrt{E}$ for hadrons, with E in GeV.

The muon system consists of rear, barrel (R/BMUON) [13] and forward (FMUON) [10] tracking detectors. The B/RMUON consists of limited-streamer (LS) tube chambers placed behind the BCAL (RCAL), inside and outside a magnetized iron yoke surrounding the CAL. The barrel and rear muon chambers cover polar angles from 34° to 135° and from 135° to 171° , respectively. The FMUON consists of six trigger planes of LS tubes and four planes of drift chambers covering the angular region from 5° to 32° . The muon system exploits the magnetic field of the iron yoke and, in the forward direction, of two iron toroids magnetized to ~ 1.6 T to provide an independent measurement of the muon momentum.

The luminosity was measured using the bremsstrahlung process $ep \rightarrow ep\gamma$. The resulting small-angle energetic photons were measured by the luminosity monitor [14], a lead-scintillator calorimeter placed in the HERA tunnel at $Z = -107$ m.

III. DATA SELECTION

The data were selected online by requiring either a high-momentum muon reaching the external B/RMUON chambers or two jets reconstructed in the CAL. A dedicated trigger requiring two jets and a muon with looser jet and muon thresholds was also used in the last part of the data taking.

Muons were reconstructed offline using the following procedure: a muon track was found in the inner and outer B/RMUON chambers or crossing at least 4 FMUON planes, then a match in position and momentum to a CTD track was required. The angular acceptance of the F/B/RMUON and of the CTD, and the requirement that the muons reach the external chambers, define three regions of good acceptance:

$$\begin{aligned} \text{rear} \quad & -1.6 < \eta^\mu < -0.9, \quad p^\mu > 2.5 \text{ GeV}; \\ \text{barrel} \quad & -0.9 < \eta^\mu < 1.3, \quad p_T^\mu > 2.5 \text{ GeV}; \\ \text{forward} \quad & 1.48 < \eta^\mu < 2.3, \quad p^\mu > 4 \text{ GeV}, \quad p_T^\mu > 1 \text{ GeV}; \end{aligned} \quad (1)$$

with the Z axis pointing in the proton beam direction, referred to as the “forward direction,” and the X axis pointing left towards the center of HERA. The coordinate origin is at the nominal interaction point.

where η^μ , p^μ , and p_T^μ are the muon pseudorapidity, momentum, and transverse momentum, respectively.

The hadronic system (including the muon) was reconstructed from energy-flow objects (EFOs) [15] which combine the information from calorimetry and tracking, corrected for energy loss in dead material. A reconstructed four-momentum $(p_X^i, p_Y^i, p_Z^i, E^i)$ was assigned to each EFO.

Jets were reconstructed from EFOs using the k_T algorithm [16] in the longitudinally invariant mode [17]. The E recombination scheme, which produces massive jets whose four-momenta are the sum of the four-momenta of the clustered objects, was used. Muons were associated with jets by the k_T algorithm: if the EFO corresponding to a reconstructed muon was included in a jet, then the muon was considered to be associated with the jet.

The event inelasticity y was reconstructed from the Jacquet–Blondel estimator $y_{\text{JB}} = (E - p_Z)/(2E_e)$ [18], where $E - p_Z = \sum_i E^i - p_Z^i$ and the sum runs over all EFOs.

A sample of events with one muon and two jets was selected by requiring

- (i) ≥ 1 muon in one of the three muon-chamber regions defined in Eq. (1);
- (ii) ≥ 2 jets with pseudorapidity $|\eta^{\text{jet}}| < 2.5$, and transverse momentum $p_T^{\text{jet}} > 7$ GeV for the highest- p_T^{jet} jet and $p_T^{\text{jet}} > 6$ GeV for the second-highest- p_T^{jet} jet;
- (iii) that the muon was associated with any jet with $p_T^{\text{jet}} > 6$ GeV and $|\eta^{\text{jet}}| < 2.5$. To assure a reliable p_T^{rel} measurement (see Sec. V), the residual jet transverse momentum, calculated excluding the associated muon, was required to be greater than 2 GeV;
- (iv) a reconstructed vertex compatible with the nominal interaction point;
- (v) no scattered-electron candidate found in the CAL;
- (vi) $0.2 < y_{\text{JB}} < 0.8$.

The last two cuts suppress background from high- Q^2 events and from non- ep interactions, and correspond to an effective cut $Q^2 < 1 \text{ GeV}^2$ and $0.2 < y < 0.8$.

After this selection, a sample of 3660 events remained.

IV. ACCEPTANCE CORRECTIONS AND BACKGROUND SIMULATION

To evaluate the detector acceptance and to provide the signal and background distributions, Monte Carlo (MC) samples of bottom, charm, and light-flavor (LF) events were generated, corresponding respectively to six, five, and three times the luminosity of the data. PYTHIA 6.2 [19,20] was used as the reference MC, and HERWIG 6.1 [21] for systematic checks. The branching ratios for direct semi-leptonic $b \rightarrow \mu X$ decays and for indirect cascade decays into muons via charm, anti-charm, τ^\pm and J/ψ , were set to $\mathcal{B}_{\text{dir}} = 0.106 \pm 0.002$ and $\mathcal{B}_{\text{indir}} = 0.103 \pm 0.007$ [22], respectively. The distribution of the decay-lepton momentum in the B-meson center-of-mass system from PYTHIA and HERWIG has been compared with measurements from e^+e^- collisions [23] and found to be in good agreement. The generated events were passed through a full simulation of the ZEUS detector based

ZEUS

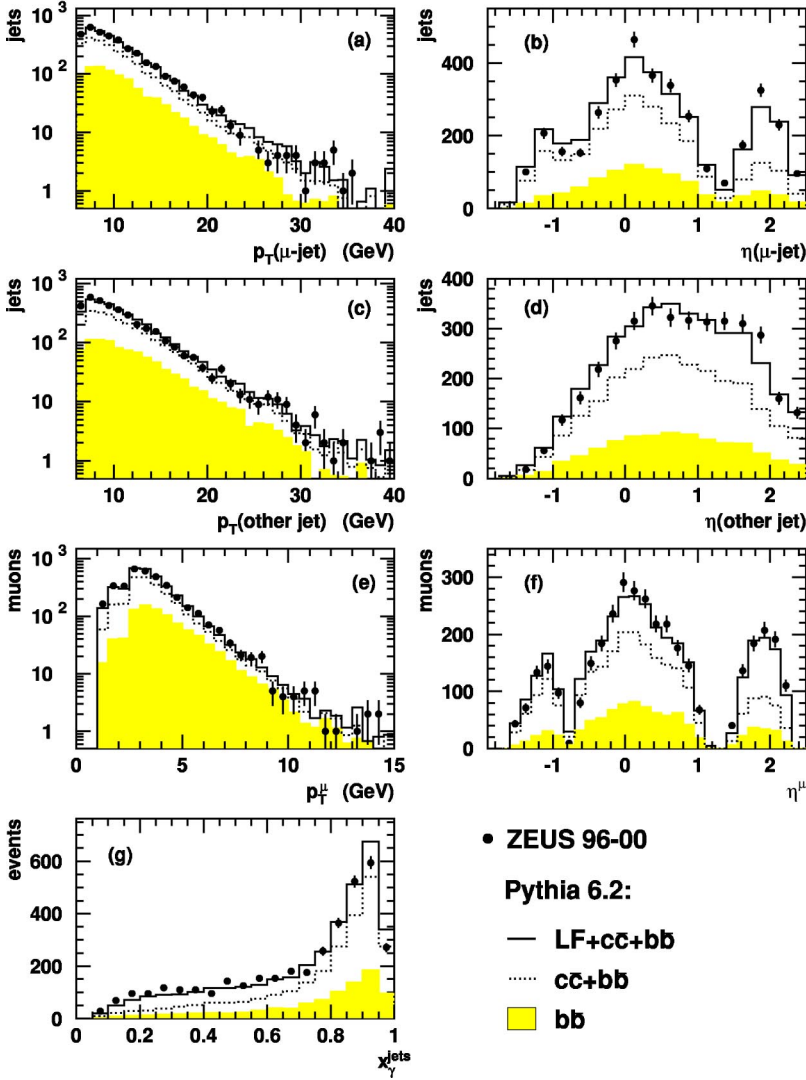


FIG. 1. Distributions for the dijet-plus-muon sample (points) compared to the predictions of the PYTHIA Monte Carlo (full line) normalized to the data. The shaded histogram shows the bottom component and the dotted line is the sum of charm and bottom. The plots show (a) the transverse momentum of the jet associated with the muon; (b) its pseudorapidity; (c) the transverse momentum of the highest- p_T non- μ -associated jet; (d) its pseudorapidity; (e) the transverse momentum of the muon; (f) its pseudorapidity; and (g) the distribution of x_γ^{jets} .

on GEANT 3.13 [24]. They were then subjected to the same trigger requirements and processed by the same reconstruction programs as for the data.

Figure 1 shows the kinematic distributions of p_T^{jet} and η^{jet} for the jet associated with the muon, as well as for highest- p_T jet that was not associated with a muon (other jet). The muon kinematic variables p_T^μ and η^μ are displayed, as well as x_γ^{jets} , the fraction of the total hadronic $E - p_Z$ carried by the two highest- p_T jets³

$$x_\gamma^{\text{jets}} = \frac{\sum_{j=1,2} (E^{\text{jet}} - p_Z^{\text{jet}})}{E - p_Z}. \quad (2)$$

³ x_γ^{jets} is the massive-jets analogue of the x_γ^{obs} variable used for massless jets in other ZEUS publications [25].

The data are compared in shape to the PYTHIA MC sample in which the relative fractions of bottom, charm, and LF were mixed according to the cross sections predicted by the simulation. The comparison shows that the main features of the dijet-plus-muon sample are well reproduced by this MC mixture. The PYTHIA MC predicts that the non- $b\bar{b}$ background comprises 57% prompt muons from charmed-hadron decays and 43% muons from light-flavor hadrons, mostly due to in-flight decays of π and K mesons, with a small amount ($\sim 5\%$ of the LF component) from muons produced in interactions with the detector material. The punch-through contribution is negligible. The HERWIG Monte Carlo (not shown) also gives a good description of the data.

The detector acceptance for the final cross sections was calculated using the $b\bar{b}$ PYTHIA Monte Carlo, in which events were reweighted such that the transverse momentum distribution of the b quark agreed with that of the NLO cal-

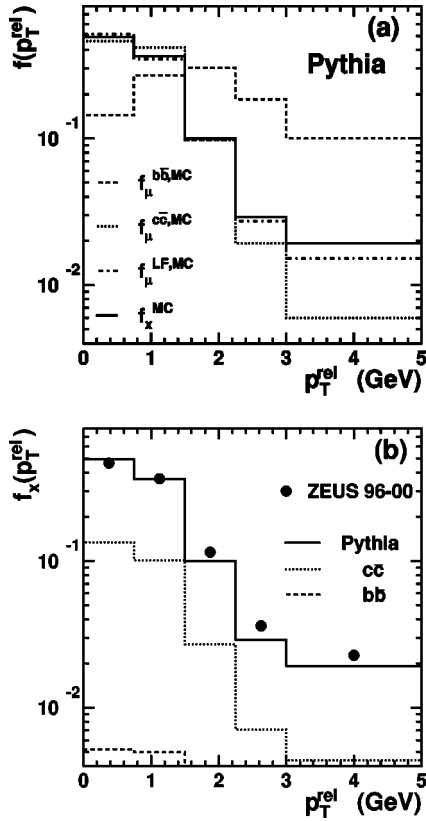


FIG. 2. (a) The p_T^{rel} distribution as predicted by the PYTHIA Monte Carlo for reconstructed muons from bottom ($f_{\mu}^{b\bar{b},\text{MC}}$, dashed histogram), charm ($f_{\mu}^{c\bar{c},\text{MC}}$, dotted histogram) and light-flavors ($f_{\mu}^{\text{LF},\text{MC}}$, dash-dotted histogram), and for unidentified tracks (f_x^{MC} , full-line histogram). The distributions are normalized to unity. (b) The p_T^{rel} distribution of unidentified data tracks (points), compared to the prediction from PYTHIA (full line). The charm and bottom components are also shown as the dotted- and dashed-line histograms, respectively.

culations. The effect of this reweighting on the distributions in Fig. 1 was small.

V. SIGNAL EXTRACTION AND CROSS SECTION MEASUREMENT

Because of the large b -quark mass, muons from semi-leptonic B-hadron decays tend to be produced with large transverse momentum with respect to the direction of the jet containing the B-hadron. The bottom signal was extracted by exploiting the distribution of the transverse momentum of the muon with respect to the momentum of the rest of the associated jet, p_T^{rel} , defined as

$$p_T^{\text{rel}} = \frac{|\mathbf{p}^{\mu} \times (\mathbf{p}^{\text{jet}} - \mathbf{p}^{\mu})|}{|\mathbf{p}^{\text{jet}} - \mathbf{p}^{\mu}|}, \quad (3)$$

where \mathbf{p}^{μ} is the muon and \mathbf{p}^{jet} the jet momentum vector. Figure 2(a) shows the distributions, normalized to unity, of the reconstructed muon p_T^{rel} as obtained from the PYTHIA MC, for bottom ($f_{\mu}^{b\bar{b},\text{MC}}$), charm ($f_{\mu}^{c\bar{c},\text{MC}}$), and LF ($f_{\mu}^{\text{LF},\text{MC}}$)

events. The p_T^{rel} distribution for bottom peaks at ~ 2 GeV and is well separated from those from charm and LF which are peaked close to zero. Since the shapes of $f_{\mu}^{\text{LF},\text{MC}}$ and $f_{\mu}^{c\bar{c},\text{MC}}$ are very similar, the fraction of bottom ($a_{b\bar{b}}$) and background (a_{bkg}) events in the sample was obtained from a two-component fit to the shape of the measured p_T^{rel} distribution f_{μ} with a bottom and a background component:

$$f_{\mu} = a_{\text{bkg}} f_{\mu}^{\text{bkg}} + a_{b\bar{b}} f_{\mu}^{b\bar{b}}, \quad (4)$$

where the p_T^{rel} distribution of bottom, $f_{\mu}^{b\bar{b}}$, was taken from the PYTHIA MC: $f_{\mu}^{b\bar{b}} = f_{\mu}^{b\bar{b},\text{MC}}$, and that of the background, f_{μ}^{bkg} , was obtained as explained below.

The distribution f_{μ}^{bkg} was obtained from the sum of a LF, f_{μ}^{LF} , and a charm, $f_{\mu}^{c\bar{c}}$, distribution weighted according to the charm fraction r obtained from the charm and LF cross sections given by PYTHIA:

$$f_{\mu}^{\text{bkg}} = r f_{\mu}^{c\bar{c}} + (1-r) f_{\mu}^{\text{LF}}. \quad (5)$$

The distribution f_{μ}^{LF} can be obtained from the p_T^{rel} distribution of a sample of CTD tracks not identified as muons but fulfilling the same momentum and angular requirements applied to muons (called “unidentified tracks” in the following). The p_T^{rel} distribution for unidentified tracks, f_x , is expected to be similar to f_{μ}^{LF} , under the assumption that the probability for an unidentified track (typically a π or a K meson) to be identified as a muon, $P_{x \rightarrow \mu}$, does not depend strongly on p_T^{rel} . This assumption is validated by the MC, since the MC distributions for the LF background, $f_{\mu}^{\text{LF},\text{MC}}$, and for the unidentified tracks, f_x^{MC} , are indeed very similar, as shown in Fig. 2a.

Figure 2(b) shows the f_x distribution obtained from a dijet sample selected without muon requirements. The shape obtained from PYTHIA, f_x^{MC} , underestimates the tail (for example, by 24% at 2.625 GeV). The p_T^{rel} shape of the LF background was therefore obtained as

$$f_{\mu}^{\text{LF}} = f_x \frac{f_{\mu}^{\text{LF},\text{MC}}}{f_x^{\text{MC}}}, \quad (6)$$

where the ratio $f_{\mu}^{\text{LF},\text{MC}}/f_x^{\text{MC}}$ is a MC-based correction that accounts for possible differences between f_{μ}^{LF} and f_x due to a residual p_T^{rel} dependence of $P_{x \rightarrow \mu}$ and to the charm and bottom contamination ($\sim 28\%$ and $\sim 2\%$ respectively) in the dijet sample.

The data cannot be used to extract the distribution $f_{\mu}^{c\bar{c}}$. Two cases were therefore considered: the distribution given by the PYTHIA MC, $f_{\mu}^{c\bar{c},\text{MC}}$, and the distribution obtained from the unidentified track sample, as in the case of the LF background: $f_x f_{\mu}^{c\bar{c},\text{MC}}/f_x^{\text{MC}}$. The average of these two cases was then taken as the nominal $f_{\mu}^{c\bar{c}}$.

Figure 3 shows the result of the p_T^{rel} fit for muons in the rear, barrel, and forward regions. The sum of the two components reproduces the data reasonably well. The fraction of b in the total sample of dijet events with a muon is $a_{b\bar{b}}$

ZEUS

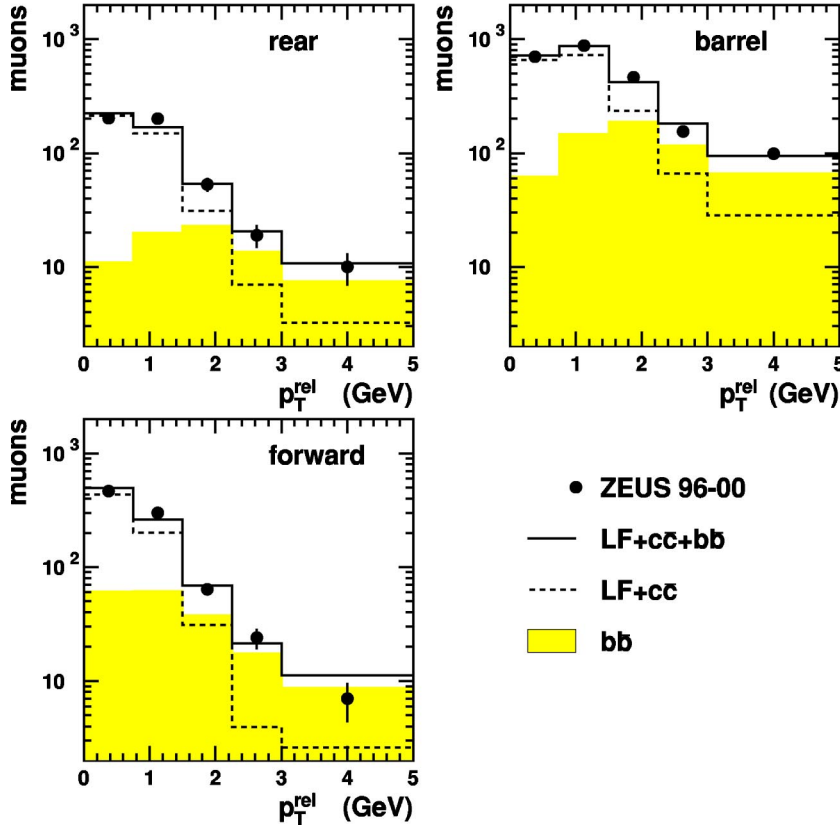


FIG. 3. The p_T^{rel} distribution for events with muons in the rear, barrel and forward regions defined in Eq. (1). The data (points) are compared to the mixture of bottom and charm+LF background obtained from the p_T^{rel} fit (full line). The shaded histogram represents the beauty component while the dashed-line histogram is the background.

$=0.224 \pm 0.017$ (stat.). In the determination of the cross sections, the fraction of beauty events in the data was extracted by a fit performed in each cross-section bin.

All the cross sections reported in Sec. VIII, with the exception of that for b quarks, are inclusive muon (or b -jet) cross sections, obtained by counting muons (or b -jets) rather than events. Muons coming from both direct and indirect b decays are considered to be part of the signal. The cross sections are given for dijet events passing the following requirements: $Q^2 < 1 \text{ GeV}^2$, $0.2 < y < 0.8$ and at least two hadron-level jets with $p_T^{\text{jet}_1} > 7 \text{ GeV}$, $p_T^{\text{jet}_2} > 6 \text{ GeV}$ and $\eta^{\text{jet}_1}, \eta^{\text{jet}_2} < 2.5$. These jets were defined using the k_T algorithm on stable hadrons, where the weakly decaying B hadrons were considered stable. For dijet events with a muon passing the cuts of Eq. (1), the acceptance varies from 10% at low p_T^μ to 20% at large p_T^μ .

The cross sections were measured from data collected at two different center-of-mass energies, $\sqrt{s} = 300 \text{ GeV}$ and $\sqrt{s} = 318 \text{ GeV}$. They were corrected to $\sqrt{s} = 318 \text{ GeV}$ using the NLO QCD prediction. The effect of this correction on the final cross section is $\sim 2\%$.

VI. THEORETICAL PREDICTIONS AND UNCERTAINTIES

The measured cross sections are compared to NLO QCD predictions based on the FMNR [26] program. The parton distribution functions used for the nominal prediction were

GRVG-HO [27] for the photon and CTEQ5M [28] for the proton. The b -quark mass was set to $m_b = 4.75 \text{ GeV}$, and the renormalization and factorization scales to the transverse mass, $\mu_r = \mu_f = m_T = \sqrt{1/2((p_T^b)^2 + (p_T^{\bar{b}})^2) + m_b^2}$, where $p_T^{b(\bar{b})}$ is the transverse momentum of the b (\bar{b}) quark in the laboratory frame. Jets were reconstructed by running the k_T algorithm on the four momenta of the b and \bar{b} quarks and of the third light parton (if present) generated by the program. The fragmentation of the b quark into a B hadron was simulated by rescaling the quark three-momentum (in the frame in which $p_Z^b = -p_Z^{\bar{b}}$, obtained with a boost along Z) according to the Peterson [29] fragmentation function with $\epsilon = 0.0035$. The muon momentum was generated isotropically in the B-hadron rest frame from the decay spectrum given by PYTHIA, which is in good agreement with measurements made at B factories [23].

To evaluate the uncertainty on the NLO calculations, the b -quark mass and the renormalisation and factorization scales were varied simultaneously, to maximize the change, from $m_b = 4.5 \text{ GeV}$ and $\mu_r = \mu_f = m_T/2$ to $m_b = 5.0 \text{ GeV}$ and $\mu_r = \mu_f = 2m_T$, producing a variation in the cross section from $+34\%$ to -22% . The effect on the cross section of a variation of the Peterson parameter ϵ from 0.002 to 0.0055 [30] and of a change of the fragmentation function from the Peterson to the Kartvelishvili parametrization (with $\alpha = 13$, as obtained from comparisons between NLO QCD and MC distributions) [31,32] was less than $\pm 3\%$. The effects of us-

ing different sets of parton densities and of a variation of the strong coupling constant ($\Lambda_{\text{QCD}}^{(5)} = 0.226 \pm 0.025$ MeV) were all within $\pm 4\%$.

The NLO cross sections, calculated for jets made of partons, were corrected for jet hadronization effects to allow a direct comparison with the measured hadron-level cross sections. The corrections were derived from the MC simulation as the ratio of the hadron-level to the parton-level MC cross section, where the parton level is defined as being the result of the parton showering stage of the simulation. The average between the corrections obtained from PYTHIA and HERWIG was taken as the central value and their difference as the uncertainty. The effect of the hadronization correction was largest in the rear region, where the cross section was reduced by $(20 \pm 6)\%$ and smallest at large p_T^μ where it was reduced by $(3.0 \pm 0.3)\%$.

The measured cross sections are also compared to the absolute predictions of two MC models, PYTHIA 6.2 and CASCADE 1.1. The predictions of PYTHIA 6.2 were obtained [20] by mixing direct- ($\gamma g \rightarrow b\bar{b}$) and resolved-photon ($gg \rightarrow b\bar{b}, q\bar{q} \rightarrow b\bar{b}$) flavor-creation processes calculated using massive matrix elements and the flavor-excitation (FE) processes ($bg \rightarrow bg, bq \rightarrow bq$), in which a heavy quark is extracted from the photon or proton parton density. The FE processes contribute about 27% of the total $b\bar{b}$ cross section. The small ($\sim 5\%$) contribution from gluon splitting in parton showers ($g \rightarrow b\bar{b}$) was not included. The parton density CTEQ4L [33] was used for the proton and GRVG-LO [27] for the photon; the b -quark mass was set to 4.75 GeV and the b -quark string fragmentation was performed according to the Peterson function with $\epsilon = 0.0041$ [34].

CASCADE [35] is a Monte Carlo implementation of the CCFM evolution equations [36]. Heavy-quark production is obtained from the $O(\alpha_s)$ matrix elements for the process $\gamma g^* \rightarrow b\bar{b}$, in which the initial gluon can be off-shell. The gluon density, unintegrated in transverse momentum (k_T), is obtained from an analysis of the proton structure functions based on the CCFM equations [37]; in the event generation the gluon density used corresponds to the set named “J2003 set 2.” The mass of the b quark was set to 4.75 GeV and α_s was evaluated at the scale m_T . As for PYTHIA, the b -quark string fragmentation was performed according to the Peterson function with $\epsilon = 0.0041$.

VII. SYSTEMATIC UNCERTAINTIES

The main experimental uncertainties are described below:

- (i) The muon acceptance, including the efficiency of the muon chambers, of the reconstruction and of the MUON-CTD matching, is known to about 10% from a study based on an independent dimuon sample [38].
- (ii) The uncertainty on the p_T^{rel} shape of the LF and charm background was evaluated by
 - (a) varying the charm fraction in the background, r , by $\pm 20\%$. This range was obtained by fixing the absolute charm-MC normalization to a measurement of the charm dijet cross section [39] and

- using the PYTHIA or HERWIG MC to extrapolate to the kinematic range of the present measurement;
- (b) varying the jet-track association in the unidentified-track sample;
- (c) extracting f_μ^{LF} from a sample of unidentified CTD tracks, reweighted with a MC-based parametrization of $P_{x \rightarrow \mu}$ depending on polar angle and momentum;
- (d) varying the p_T^{rel} shape of the charm component of the background between the prediction from PYTHIA and the value obtained from the unidentified track sample;
- (e) using HERWIG instead of PYTHIA to simulate the background.

The total uncertainty from these sources is about 10%. As a cross-check, a different definition of p_T^{rel} was used to extract the beauty fraction, namely the transverse momentum of the muon with respect to the whole jet, including the muon itself, as used in a previous ZEUS publication [9]. The results were found to be in good agreement:

- (iii) The 2% uncertainty on the direct-decay branching ratio \mathcal{B}_{dir} introduces a 2% uncertainty on the b -jet and on the b -quark cross sections while it has no effect on the visible muon cross sections. The 7% uncertainty on the branching ratio for indirect decays $\mathcal{B}_{\text{indir}}$ produces an uncertainty of 1% on the measured cross sections.
- (iv) The uncertainties on the dijet selection, on the energy scale, on the jet and y_{JB} resolution and trigger efficiency add up to a 7% uncertainty on the cross sections.

The uncertainty arising from the model dependence of the acceptance was evaluated as follows (the effect on the cross sections is shown in parenthesis):

- (v) The Peterson fragmentation parameter ϵ in the MC was varied from 0.002 to 0.006 as allowed by LEP and SLD measurements [34,40,41]. The Lund–Bowler fragmentation function was used as an alternative, both with the default PYTHIA parameters and with parameters taken from OPAL measurements [34] ($\pm 2\%$).
- (vi) Instead of using PYTHIA reweighted to the NLO p_T^b distribution it was reweighted as a function of η^{jet} and p_T^{jet} to agree with the measured differential distributions (-2%) or without reweighting ($+2\%$).
- (vii) The fraction of flavor-excitation events in PYTHIA was varied up and down by a factor of 2 ($\pm 4\%$), as allowed by comparisons to the x_γ^{jets} distribution of the data.
- (viii) HERWIG was used instead of PYTHIA (-2%).

The total systematic uncertainty was obtained by adding the above contributions in quadrature. A 2% overall normalization uncertainty associated with the luminosity measurement was not included.

VIII. RESULTS

All the cross sections reported below, except for the b -quark cross section, are given for dijet events with $p_T^{\text{jet}_1}$,

ZEUS

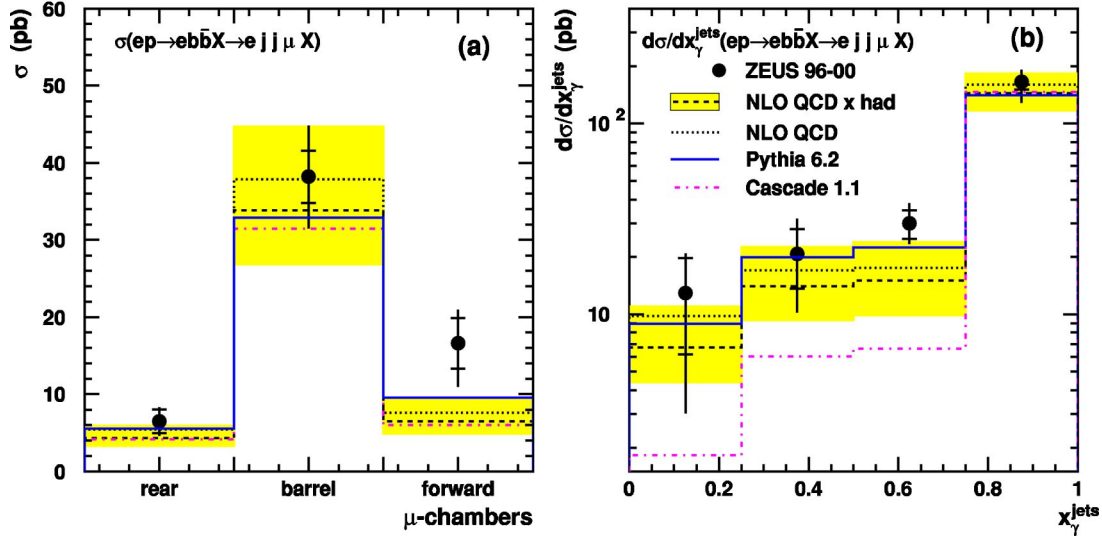


FIG. 4. Cross sections for muons coming from b decays in dijet events with $p_T^{\text{jet}_1} > 7$, $p_T^{\text{jet}_2} > 6$ GeV, $\eta^{\text{jet}_1}, \eta^{\text{jet}_2} < 2.5$, $0.2 < y < 0.8$, $Q^2 < 1$ GeV² passing the selection of Eq. (1). (a) The cross section for the forward, barrel and rear regions [defined in Eq. (1)]. (b) The differential cross section as a function of x_γ^{jets} . The data (points) are compared to the predictions of NLO QCD (dotted line: parton-level jets; dashed line: jets corrected to the hadron level). The full error bars are the quadratic sum of the statistical (inner part) and systematic uncertainties. The band around the NLO prediction represents the variation on the theoretical predictions obtained by varying the b -quark mass, μ_r and μ_f , as explained in the text. The data are also compared to the predictions of the PYTHIA (solid line histogram) and CASCADE (dot-dashed line histogram) Monte Carlo models.

$p_T^{\text{jet}_2} > 7$, 6 GeV, $\eta^{\text{jet}_1}, \eta^{\text{jet}_2} < 2.5$, $Q^2 < 1$ GeV², and $0.2 < y < 0.8$.

The first set of measurements are bottom cross sections for muons passing the cuts defined in Eq. (1). The results for the forward, barrel, and rear muon-chamber regions are shown in Fig. 4(a) and Table I and compared with the NLO prediction and MC models. Both the NLO and the MC models are in reasonable agreement with the data.

Figure 4(b) and Table II show the differential cross-section $d\sigma/dx_\gamma^{\text{jets}}$ for muons in the range defined by Eq. (1) in dijet events. The x_γ^{jets} variable corresponds at leading order to the fraction of the exchanged-photon momentum in the hard scattering process. It provides a tool to measure the relative importance of photon-gluon fusion, $\gamma g \rightarrow b\bar{b}$, which gives a peak at $x_\gamma^{\text{jets}} \sim 1$, and of other contributions, such as gluon-

gluon fusion (with a gluon coming from the photon) or higher-order diagrams, which are distributed over the whole x_γ^{jets} range. The sample is dominated by the high- x_γ^{jets} peak, but a low- x_γ^{jets} component is also apparent. The NLO QCD prediction describes the distribution well. PYTHIA is also able to give a good description of the data due to the large contribution from flavor excitation at low x_γ^{jets} . CASCADE, which generates low- x_γ^{jets} events via initial-state radiation without using a parton density in the photon, tends to underestimate the cross section at low x_γ^{jets} .

The differential cross sections in the muonic variables were measured for $p_T^\mu > 2.5$ GeV and $-1.6 < \eta^\mu < 2.3$. Figure 5 and Table III show the differential cross sections $d\sigma/d\eta^\mu$ and $d\sigma/dp_T^\mu$ for muons in dijet events. The NLO QCD predictions and the MC models describe the η^μ distribution well. The p_T^μ distribution is well reproduced by NLO

TABLE I. For each muon-chamber region defined in Eq. (1) the columns show the number of selected muons; the beauty fraction $a_{b\bar{b}}$ obtained from the p_T^{rel} fit; the measured bottom cross section with the statistical and systematic uncertainties; the NLO QCD prediction corrected to the hadron level with the theoretical uncertainty and the hadronization correction. For further details see the caption to Fig. 4.

μ -chambers	Muons	$a_{b\bar{b}}$	$\sigma \pm \text{stat.} \pm \text{syst.}$ (pb)	$\sigma^{\text{NLO}} \times C_{\text{had}}$ (pb)	C_{had}
rear	484	0.15	$6.5 \pm 1.5^{+1.0}_{-1.1}$	$4.3^{+1.6}_{-1.0}$	0.80
barrel	2316	0.25	$38.2 \pm 3.4^{+5.7}_{-5.8}$	$33.9^{+11.0}_{-7.0}$	0.89
forward	868	0.21	$16.6 \pm 3.3^{+2.9}_{-4.6}$	$6.5^{+2.8}_{-1.6}$	0.86

TABLE II. Differential muon cross section as a function of x_γ^{jets} . The multiplicative hadronization correction applied to the NLO prediction is shown in the last column. For further details see the caption to Fig. 4.

x_γ^{jets} range	$d\sigma/dx_\gamma^{\text{jets}} \pm \text{stat.} \pm \text{syst.}$ (pb)	C_{had}
0.00, 0.25	$12.9 \pm 6.7^{+4.2}_{-7.2}$	0.68
0.25, 0.50	$20.8 \pm 7.2^{+8.2}_{-7.7}$	0.83
0.50, 0.75	$30.0 \pm 5.2^{+6.4}_{-4.1}$	0.86
0.75, 1.00	$165 \pm 14^{+22}_{-34}$	0.90

ZEUS

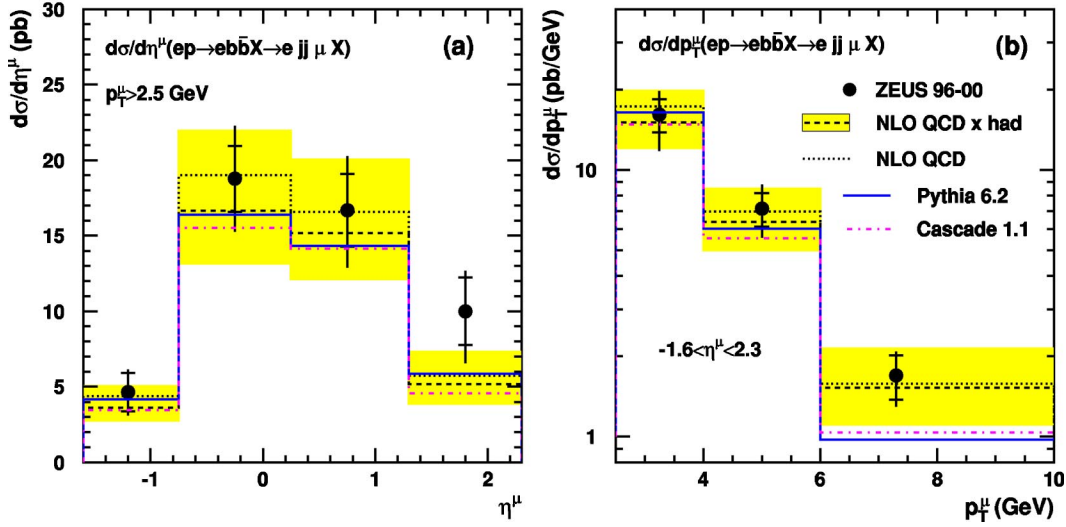


FIG. 5. Differential cross sections as a function of (a) the muon pseudorapidity η^μ and (b) transverse momentum p_T^μ , for $p_T^\mu > 2.5$ GeV and $-1.6 < \eta^\mu < 2.3$, for muons coming from b decays in dijet events with $p_T^{\text{jet}_1} > 7$, $p_T^{\text{jet}_2} > 6$ GeV, η^{jet_1} , $\eta^{\text{jet}_2} < 2.5$, $0.2 < y < 0.8$, $Q^2 < 1$ GeV². The data (points) are compared to the predictions of NLO QCD (dotted line: parton-level jets; dashed line: corrected to hadron-level jets). The full error bars are the quadratic sum of the statistical (inner part) and systematic uncertainties. The band around the NLO prediction represents the variation on the theoretical predictions obtained by varying the b -quark mass and μ_r and μ_f as explained in the text. The data are also compared to the predictions of the PYTHIA (solid line histogram) and CASCADE (dot-dashed line histogram) Monte Carlo models.

QCD while the p_T^μ slope tends to be too soft in CASCADE and PYTHIA.

The jet associated with the muon (or μ -jet) reproduces the kinematics of the b (or \bar{b}) quark to a good approximation. The μ -jet is defined as the jet containing the B hadron that decays into the muon. Figures 6(a) and 6(b) and Table IV show the differential cross section for the jet associated with a muon passing the cuts of Eq. (1) as a function of the jet pseudorapidity, $d\sigma/d\eta^{\mu\text{-jet}}$, and transverse momentum, $d\sigma/dp_T^{\mu\text{-jet}}$, for $\eta^{\mu\text{-jet}} < 2.5$ and $p_T^{\mu\text{-jet}} > 6$ GeV. The μ -jet distributions are well reproduced by the NLO and by the MC models.

The μ -jet cross sections have been corrected to obtain the

TABLE III. Differential muon cross section as a function of η^μ and p_T^μ . For further details see the caption to Fig. 5.

η^μ range	$d\sigma/d\eta^\mu \pm \text{stat.} \pm \text{syst.}$ (pb)	C_{had}
-1.6, -0.75	$4.6 \pm 1.3^{+0.8}_{-0.9}$	0.83
-0.75, 0.25	$18.8 \pm 2.2^{+2.7}_{-2.7}$	0.88
0.25, 1.30	$16.7 \pm 2.4^{+2.7}_{-2.9}$	0.92
1.30, 2.30	$10.0 \pm 2.3^{+1.4}_{-2.6}$	0.91
p_T^μ range (GeV)	$d\sigma/dp_T^\mu \pm \text{stat.} \pm \text{syst.}$ (pb/GeV)	C_{had}
2.5, 4.0	$16.1 \pm 2.3^{+2.9}_{-3.7}$	0.87
4.0, 6.0	$7.1 \pm 1.0^{+1.3}_{-1.2}$	0.92
6.0, 10.0	$1.69 \pm 0.32^{+0.22}_{-0.24}$	0.97

cross sections for b -jets in dijet events: $\sigma(ep \rightarrow e' jjX)$. A b -jet is defined as a jet containing a B (or an anti- B) hadron. This correction was performed using PYTHIA and accounts for the $b \rightarrow \mu$ branching ratio, including direct and indirect decays, and for the full muon phase space. Figures 6(c) and 6(d) and Table V show the differential cross-sections $d\sigma/d\eta^{b\text{-jet}}$ and $d\sigma/dp_T^{b\text{-jet}}$. The level of agreement of b jets with the NLO QCD and MC predictions is similar to that found for the μ jets. It should be noted that the hadronization corrections in the first two $\eta^{b\text{-jet}}$ bins are large ($\sim -20\%$).

To compare the present result with a previous ZEUS measurement given at the b -quark level, the NLO QCD prediction was used to extrapolate the cross section for dijet events with a muon to the inclusive b -quark cross section. The b -quark differential cross section as a function of the quark transverse momentum, $d\sigma(ep \rightarrow bX)/dp_T^b$, for b -quark pseudo-rapidity in the laboratory frame $|\eta^b| < 2$ (corresponding to a rapidity in the ep center of mass of $-3.75 < Y_{\text{cms}}^b < 0.25$), for $Q^2 < 1$ GeV² and $0.2 < y < 0.8$, was obtained from the dijet cross section for events with a μ -jet within $|\eta^{\mu\text{-jet}}| < 2$ using the NLO prediction corrected for hadronization. The \bar{b} quark was not considered in the definition of the b -quark cross section. As a cross-check, the measurement was corrected to the b -quark level using the PYTHIA MC, giving a result in agreement within 6%. The result, shown in Fig. 7 and Table VI, is compared to the previous ZEUS measurement [9] of the b -quark cross section for $p_T^b > p_T^{\text{min}} = 5$ GeV and $|\eta^b| < 2$, translated into a differential cross section using the NLO prediction and plotted at the average b -quark transverse momentum, $\langle p_T^b \rangle$, of the accepted events taken from the Monte Carlo:

ZEUS

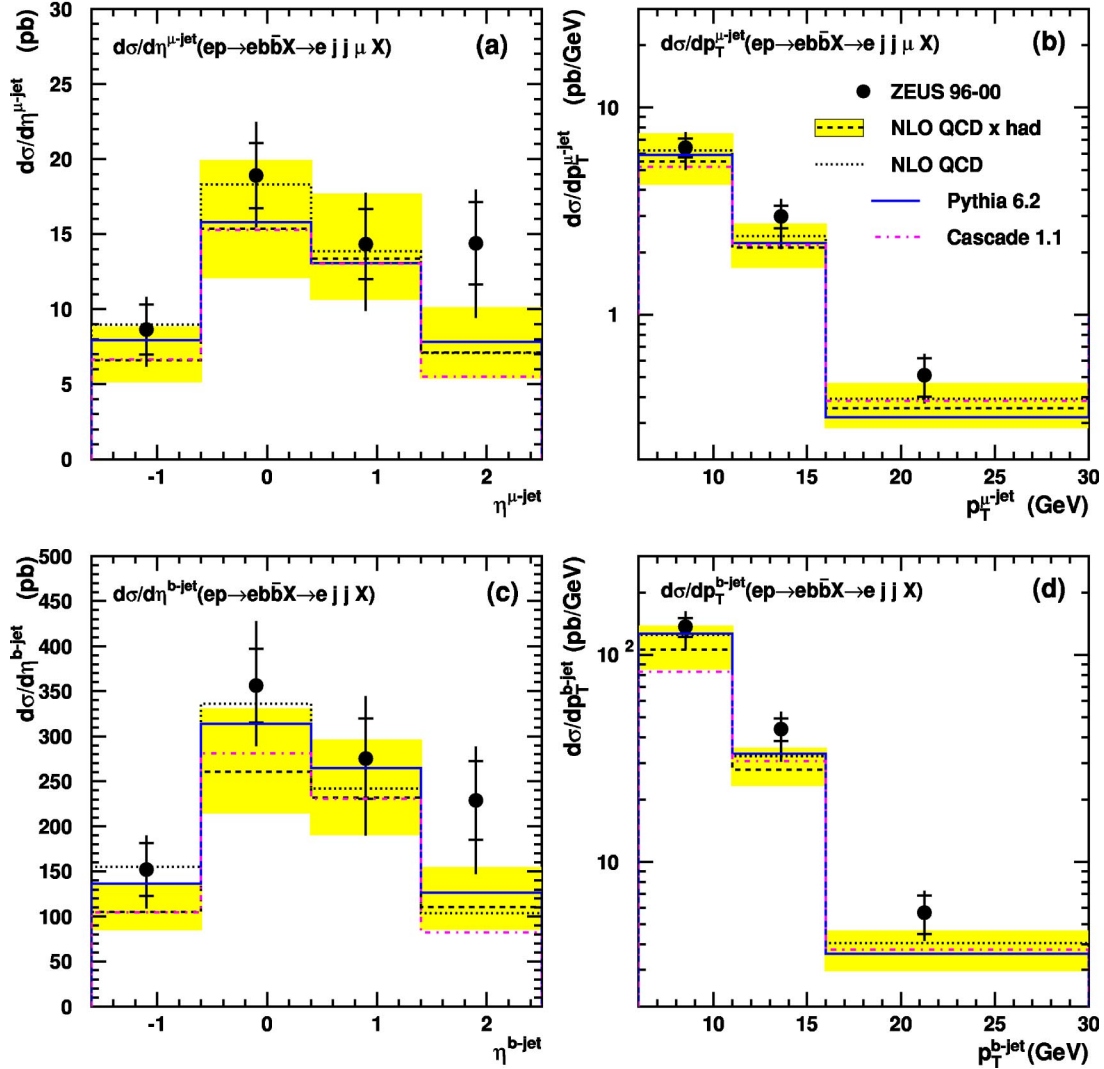


FIG. 6. Differential cross sections as a function of (a) the pseudorapidity $\eta^{\mu\text{-jet}}$ and (b) the transverse momentum $p_T^{\mu\text{-jet}}$ of the jet associated to the muon, for $p_T^{\mu\text{-jet}} > 6$ GeV, $\eta^{\mu\text{-jet}} < 2.5$, for muons passing the selection of Eq. (1) and coming from b decays; differential cross sections as a function of (c) the pseudorapidity $\eta^{b\text{-jet}}$ and (d) the transverse momentum $p_T^{b\text{-jet}}$ of the jet containing a B hadron. All the cross sections are evaluated for dijet events with $p_T^{\text{jet1}} > 7$, $p_T^{\text{jet2}} > 6$ GeV, $\eta^{\text{jet1}}, \eta^{\text{jet2}} < 2.5$, $0.2 < y < 0.8$, $Q^2 < 1$ GeV². The data (points) are compared to the predictions of NLO QCD (dotted line: parton level; dashed line: corrected to hadron level). The full error bars are the quadratic sum of the statistical (inner part) and systematic uncertainties. The band around the NLO prediction represents the uncertainty on the theoretical prediction corrected for hadronization. The data are also compared to the predictions of the PYTHIA (solid line histogram) and CASCADE (dot-dashed line histogram) Monte Carlo models.

$$\left(\frac{d\sigma}{dp_T^b} \right)_{\langle p_T^b \rangle} = \left(\frac{d\sigma^{\text{NLO}}}{dp_T^b} \right)_{\langle p_T^b \rangle} \frac{\sigma(p_T^b > p_T^{\text{min}})}{\sigma^{\text{NLO}}(p_T^b > p_T^{\text{min}})}.$$

The two independent measurements are consistent and in agreement with the NLO QCD predictions.

IX. CONCLUSIONS

Bottom production identified by semi-leptonic decay into muons has been measured in dijet events with $Q^2 < 1$ GeV². Differential cross sections for the reaction $ep \rightarrow e' b \bar{b} X \rightarrow e' j j \mu X'$ have been measured as a function of

the pseudorapidity and transverse momentum of the muon and of x_γ^{jets} . Differential cross sections for the production of b -jets were also measured.

The results were compared to MC models and to a NLO QCD prediction combined with fragmentation and B -hadron decay models. This prediction is in good agreement with the data in all the differential distributions. The PYTHIA MC model is also able to give a reasonable description of the differential cross sections. The CASCADE MC model also gives a reasonable description of the data, except for the low- x_γ^{jets} region.

The large excess of the first measurement of bottom photoproduction over NLO QCD, reported by the H1 collabora-

TABLE IV. Differential cross section for jets associated with a muon as a function of $\eta^{\mu\text{-jet}}$ and $p_T^{\mu\text{-jet}}$. For further details see the caption to Fig. 6.

$\eta^{\mu\text{-jet}}$ range	$d\sigma/d\eta^{\mu\text{-jet}} \pm \text{stat.} \pm \text{syst.}$ (pb)	C_{had}
-1.6, -0.6	$8.6 \pm 1.7^{+1.4}_{-1.8}$	0.73
-0.6, 0.4	$18.9 \pm 2.2^{+2.8}_{-2.7}$	0.84
0.4, 1.4	$14.3 \pm 2.3^{+2.5}_{-3.8}$	0.97
1.4, 2.5	$14.4 \pm 2.7^{+2.3}_{-4.2}$	1.00
$p_T^{\mu\text{-jet}}$ range (GeV)	$d\sigma/dp_T^{\mu\text{-jet}} \pm \text{stat.} \pm \text{syst.}$ (pb/GeV)	C_{had}
6, 11	$6.41 \pm 0.67^{+1.00}_{-1.24}$	0.88
11, 16	$2.98 \pm 0.37^{+0.52}_{-0.82}$	0.88
16, 30	$0.51 \pm 0.11^{+0.08}_{-0.08}$	0.90

tion [8], is not confirmed. The present result is consistent with the previous ZEUS measurement using semi-leptonic B decays into electrons [9]. Beauty photoproduction in ep collisions is reasonably well described both by NLO QCD and by a MC model that includes a substantial flavor excitation component.

ACKNOWLEDGMENTS

We thank the DESY Directorate for their strong support and encouragement. The remarkable achievements of the HERA machine group were essential for the successful completion of this work and are greatly appreciated. We are grateful for the support of the DESY computing and network services. The design, construction, and installation of the ZEUS detector have been made possible owing to the ingenuity and effort of many people who are not listed as authors. It is also a pleasure to thank S. Frixione and H. Jung for help with theoretical predictions and useful conversation. IG-B was partly supported by Polish Ministry of Scientific Re-

TABLE V. Differential cross section for b -jets as a function of $\eta^{b\text{-jet}}$ and $p_T^{b\text{-jet}}$. For further details see the caption to Fig. 6.

$\eta^{b\text{-jet}}$ range	$d\sigma/d\eta^{b\text{-jet}} \pm \text{stat.} \pm \text{syst.}$ (pb)	C_{had}
-1.6, -0.6	$152 \pm 29^{+24}_{-31}$	0.68
-0.6, 0.4	$356 \pm 41^{+59}_{-53}$	0.78
0.4, 1.4	$275 \pm 45^{+53}_{-73}$	0.96
1.4, 2.5	$229 \pm 44^{+41}_{-69}$	1.06
$p_T^{b\text{-jet}}$ range (GeV)	$d\sigma/dp_T^{b\text{-jet}} \pm \text{stat.} \pm \text{syst.}$ (pb/GeV)	C_{had}
6, 11	$137 \pm 14^{+21}_{-27}$	0.85
11, 16	$43.8 \pm 5.5^{+7.7}_{-12.0}$	0.86
16, 30	$5.7 \pm 1.2^{+1.0}_{-0.9}$	0.89

search and Information Technology, Grant No. 2P03B 122 25. JS was partly supported by the Israel Science Foundation and the Ministry of Science, and Polish Ministry of Scientific Research and Information Technology, Grant No. 2P03B12625. AK was supported by the Polish State Committee for Scientific Research, Grant No. 2 P03B09322. BBL was partly supported by the Russian Foundation for Basic Research, Grant No. 02-02-81023. RC was supported by the Polish State Committee for Scientific Research, Grant No. 2 P03B07222. J. S. (Warsaw University) was supported by the KBN Grant No. 2P03B12925. TT and AU were supported by German Federal Ministry for Education and Research (BMBF), POL 01/043. JU was supported by the KBN Grant No. 2P03B12725. LKG was partly supported by University of Wisconsin via the U.S.-Israel BSF. McGill University, University of Toronto, and York University were supported by the Natural Sciences and Engineering Research Council of Canada (NSERC). Physikalisches Institut der Universität Bonn, and the Institute of Exp. Physics at Hamburg University were supported by the German Federal Ministry for Education and Research (BMBF), under Contract Nos. HZ1GUA

ZEUS

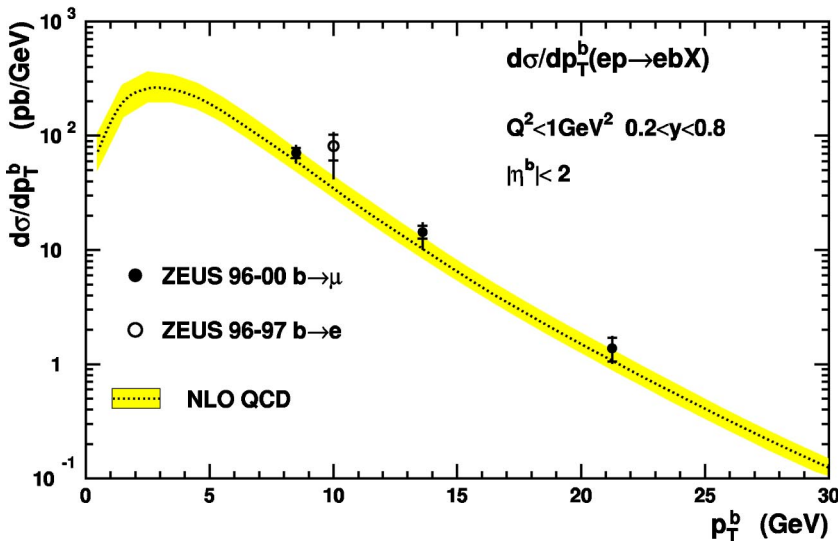


FIG. 7. Differential cross section for b -quark production as a function of the b -quark transverse momentum p_T^b for b -quark pseudorapidity $|\eta^b| < 2$ and for $Q^2 < 1 \text{ GeV}^2$, $0.2 < y < 0.8$. The filled points show the ZEUS results from this analysis and the open point is the previous ZEUS measurement in the electron channel [9]. The full error bars are the quadratic sum of the statistical (inner part) and systematic uncertainties. The dashed line shows the NLO QCD prediction with the theoretical uncertainty shown as the shaded band.

TABLE VI. Differential b -quark cross-section $d\sigma/dp_T^b$. The first columns show the differential μ -jet cross-section $d\sigma/dp_T^{\mu\text{-jet}}$ restricted to $|\eta^{\mu\text{-jet}}| < 2$, the corresponding hadronization correction and the average b -quark transverse momentum, $\langle p_T^b \rangle$, as obtained from the PYTHIA MC. The b -quark differential cross section $d\sigma/dp_T^b$ for $|\eta^b| < 2$, evaluated at $\langle p_T^b \rangle$, is shown in the last column. For further details see the caption to Fig. 7.

$p_T^{\mu\text{-jet}}$ range (GeV)	$d\sigma/dp_T^{\mu\text{-jet}} \pm \text{stat.} \pm \text{syst.}$ ($ \eta^{\mu\text{-jet}} < 2$) (pb/GeV)	C_{had}	$\langle p_T^b \rangle$ (GeV)	$d\sigma/dp_T^b \pm \text{stat.} \pm \text{syst.}$ (pb/GeV)
6, 11	$6.22 \pm 0.63^{+0.91}_{-1.04}$	0.87	8.5	$70 \pm 7.2^{+13}_{-14}$
11, 16	$2.74 \pm 0.36^{+0.47}_{-0.74}$	0.88	13.6	$14.4 \pm 1.9^{+3.1}_{-4.3}$
16, 30	$0.43 \pm 0.10^{+0.07}_{-0.06}$	0.88	21.25	$1.37 \pm 0.32^{+0.39}_{-0.37}$

2, HZ1GUB 0, HZ1PDA 5, and HZ1VFA 5. Weizmann Institute, Rehuvut, Israel was supported by the MINERVA Gesellschaft für Forschung GmbH, the Israel Science Foundation, the U.S.-Israel Binational Science Foundation and the Benozio Center for High Energy Physics. Tel. Aviv University was supported by the German-Israeli Foundation and the Israel Science Foundation. Calabria University Physics Department and Dipartimento di Fisica dell'Università, Università 'La Sapienza,' Università di Torino, and Università del Piemonte Orientale were supported by the Italian National Institute for Nuclear Physics (INFN). The Institute of Particle and Nuclear Physics, Meiji Gakuin University, Polytechnic Institute, Tokyo Institute of Technology, University of Tokyo, and Tokyo Metropolitan University were supported by the Japanese Ministry of Education, Culture, Sports, Science and Technology (MEXT) and its grants for Scientific Research. Chonnam National University and Kyungpook National University were supported by the Korean Ministry of Education and Korea Science and Engineering Foundation. NIKHEF and University of Amsterdam were supported by the Netherlands Foundation for Research on Matter (FOM). The Institute of Nuclear Physics, Cracow, was supported by the Polish State Committee for Scientific Research, Grant No. 620/E-77/SPB/DESY/P-03/DZ 117/2003-2005. Moscow Engineering Institute was partially supported by the German Federal Ministry for Education and

Research (BMBF). Moscow State University was partly supported by the Russian Ministry of Industry, Science and Technology through its grant for Scientific Research on High Energy Physics. Universidad Autonoma de Madrid was supported by the Spanish Ministry of Education and Science through funds provided by CICYT. H. H. Wills Physics Laboratory at University of Bristol, the Department of Physics and Astronomy at the University of Glasgow, the High Energy Nuclear Physics Group at Imperial College London, University of Oxford, Rutherford Appleton Laboratory, University College London were supported by the Particle Physics and Astronomy Research Council, UK. Argonne National Laboratory, Ohio State University, University of California—Santa Cruz, University of Wisconsin, and Yale University were supported by the U.S. Department of Energy. Nevis Laboratories at Columbia University and the Pennsylvania State University were supported by the US National Science Foundation. AGH—University of Science and Technology, Cracow, was supported by the Polish State Committee for Scientific Research, Grant No. 112/E-356/SPUB/DESY/P-03/DZ 116/2003-2005, 2 P03B 13922. Warsaw University, Institute of Experimental Physics and Institute for Nuclear Physics were supported by the Polish State Committee for Scientific Research, Grant No. 115/E-343/SPUB-M/DESY/P-03/DZ 121/2001-2002, 2 P03B 07022.

- [1] S. Frixione *et al.*, Nucl. Phys. **B454**, 3 (1995); M. Cacciari, S. Frixione, and P. Nason, J. High Energy Phys. **03**, 006 (2001).
- [2] M. Basile *et al.*, Lett. Nuovo Cimento Soc. Ital. Fis. **31**, 97 (1981).
- [3] UA1 Collaboration, C. Albajar *et al.*, Phys. Lett. B **256**, 121 (1991); erratum **262**, 497 (1991); Z. Phys. C **61**, 41 (1994).
- [4] CDF Collaboration, F. Abe *et al.*, Phys. Rev. Lett. **71**, 500 (1993); **71**, 2396 (1993); **75**, 1451 (1995); Phys. Rev. D **53**, 1051 (1996); CDF Collaboration, P. Acosta *et al.*, *ibid.* **65**, 052005 (2002); DØ Collaboration, S. Abachi *et al.*, Phys. Rev. Lett. **74**, 3548 (1995); DØ Collaboration, B. Abbott *et al.*, Phys. Lett. B **487**, 264 (2000); Phys. Rev. Lett. **84**, 5478 (2000); **85**, 5068 (2000).
- [5] L3 Collaboration, M. Acciarri *et al.*, Phys. Lett. B **503**, 10 (2001).
- [6] WA78 Collaboration, M. Catanesi *et al.*, Phys. Lett. B **202**, 453 (1988); E672/E706 Collaboration, R. Jesik *et al.*, Phys. Rev. Lett. **74**, 495 (1995).
- [7] E771 Collaboration, T. Alexopoulos *et al.*, Phys. Rev. Lett. **82**, 41 (1999); D. M. Jansen *et al.*, *ibid.* **74**, 3118 (1995); HERA-B Collaboration, I. Abt *et al.*, Eur. Phys. J. C **26**, 345 (2003).
- [8] H1 Collaboration, C. Adloff *et al.*, Phys. Lett. B **467**, 156 (1999); Erratum **518**, 331 (2001).
- [9] ZEUS Collaboration, J. Breitweg *et al.*, Eur. Phys. J. C **18**, 625 (2001).
- [10] ZEUS Collaboration, U. Holm (ed.), *The ZEUS Detector*. Status Report (unpublished), DESY (1993), available on <http://www-zeus.desy.de/bluebook/bluebook.html>.
- [11] N. Harnew *et al.*, Nucl. Instrum. Methods Phys. Res. A **279**, 290 (1989); B. Foster *et al.*, Nucl. Phys. Proc. Suppl. B **32**, 181 (1993); B. Foster *et al.*, Nucl. Instrum. Methods Phys. Res. A **338**, 254 (1994).

- [12] M. Derrick *et al.*, Nucl. Instrum. Methods Phys. Res. A **309**, 77 (1991); A. Andresen *et al.*, *ibid.* **309**, 101 (1991); A. Caldwell *et al.*, *ibid.* **321**, 356 (1992); A. Bernstein *et al.*, *ibid.* **336**, 23 (1993).
- [13] G. Abbiendi *et al.*, Nucl. Instrum. Methods Phys. Res. A **333**, 342 (1993).
- [14] J. Andruszków *et al.*, preprint DESY-92-066, DESY, 1992; ZEUS Collaboration, M. Derrick *et al.*, Z. Phys. C **63**, 391 (1994); J. Andruszków *et al.*, Acta Phys. Pol. B **32**, 2025 (2001).
- [15] ZEUS Collaboration, J. Breitweg *et al.*, Eur. Phys. J. C **1**, 81 (1998); G. M. Briskin, Ph.D. thesis, Tel Aviv University (1998), DESY-THESIS-1999-036.
- [16] S. Catani, Yu. L. Dokshitzer, and B. R. Webber, Phys. Lett. B **285**, 291 (1992).
- [17] S. D. Ellis and D. E. Soper, Phys. Rev. D **48**, 3160 (1993).
- [18] F. Jacquet and A. Blondel, *Proceedings of the Study for an ep Facility for Europe*, edited by U. Amaldi, Hamburg, Germany (1979), p. 391. Also in preprint DESY 79/48.
- [19] T. Sjöstrand *et al.*, Comput. Phys. Commun. **138**, 238 (2001).
- [20] E. Norrbin and T. Sjöstrand, Eur. Phys. J. C **17**, 137 (2000).
- [21] G. Marchesini *et al.*, Comput. Phys. Commun. **67**, 465 (1992).
- [22] Particle Data Group, K. Hagiwara *et al.*, Phys. Rev. D **66**, 010001 (2002).
- [23] Belle Collaboration, K. Abe *et al.*, Phys. Lett. B **547**, 181 (2002); Babar Collaboration, B. Aubert *et al.*, Phys. Rev. D **67**, 031101 (2003).
- [24] R. Brun *et al.*, GEANT3, Technical Report CERN-DD/EE/84-1, CERN, 1987.
- [25] ZEUS Collaboration, M. Derrick *et al.*, Phys. Lett. B **348**, 665 (1995).
- [26] S. Frixione *et al.*, Nucl. Phys. **B412**, 225 (1994).
- [27] M. Gluck, E. Reya, and A. Vogt, Phys. Rev. D **46**, 1973 (1992).
- [28] CTEQ Collaboration, H. L. Lai *et al.*, Eur. Phys. J. C **12**, 375 (2000).
- [29] C. Peterson *et al.*, Phys. Rev. D **27**, 105 (1983).
- [30] P. Nason and C. Oleari, Nucl. Phys. **B565**, 245 (2000).
- [31] V. G. Kartvelishvili, A. K. Likhoded, and V. A. Petrov, Phys. Lett. B **78**, 615 (1978).
- [32] M. Cacciari and P. Nason, Phys. Rev. Lett. **89**, 122003 (2002).
- [33] H. L. Lai *et al.*, Phys. Rev. D **55**, 1280 (1997).
- [34] OPAL Collaboration, G. Abbiendi *et al.*, Eur. Phys. J. C **29**, 463 (2003).
- [35] H. Jung and G. P. Salam, Eur. Phys. J. C **19**, (2001); H. Jung, Comput. Phys. Commun. **143**, 100 (2002).
- [36] M. Ciafaloni, Nucl. Phys. **B296**, 49 (1998); S. Catani, F. Fiorani, and G. Marchesini, Phys. Lett. B **234**, 339 (1990).
- [37] M. Hansson and H. Jung, preprint hep/ph0309009.
- [38] M. Turcato, Ph.D. thesis, Padova University, (2002), DESY-THESIS-2003-039.
- [39] ZEUS Collaboration, S. Chekanov *et al.*, Phys. Lett. B **565**, 87 (2003).
- [40] ALEPH Collaboration, A. Heister *et al.*, Phys. Lett. B **512**, 30 (2001).
- [41] SLD Collaboration, K. Abe *et al.*, Phys. Rev. D **65**, 092006 (2002); Erratum **66**, 079905 (2002).